Eur. Phys. J. Special Topics **229**, 2923–2935 (2020)

https://doi.org/10.1140/epjst/e2020-000113-3

THE EUROPEAN
PHYSICAL JOURNAL
SPECIAL TOPICS

Regular Article

How the shift in the phase transition temperature influences the evolution of crystals during the intermediate stage of phase transformations

Eugenya V. Makoveeva[a] and Dmitri V. Alexandrov

Department of Theoretical and Mathematical Physics, Laboratory of Multi-Scale Mathematical Modeling, Ural Federal University, Lenin avenue 51, Ekaterinburg 620000, Russia

Received 12 June 2020 / Accepted 11 September 2020

Abstract. The influence of the phase transition temperature shift on the growth dynamics of a polydisperse ensemble of spherical crystals in metastable melts and solutions is studied. This shift is connected with the Gibbs–Thomson effect and the attachment kinetics of atoms at the phase transition interfaces of evolving crystals. The nonlinear model of kinetic and balance equations with allowance for the particle "diffusion" term is solved analytically. The obtained solution is compared with the case when this temperature shift is not taken into account. It is shown that the Gibbs–Thomson and attachment kinetics effects slightly accelerate the system desupercooling for a single-component titanium melt. This shifts the particle-size distribution function and changes the shape of its tail, which is responsible for the concluding stage of Ostwald ripening.

1 Introduction

It is well-known that the growth of crystals from metastable melts and solutions frequently met in natural phenomena and different areas of applied science [1–6]. Such processes are also a powerful tool in the production of crystals of given sizes and properties in the chemical and food industries, as well as in the synthesis of certain drugs [7–13]. A wide range of applications of crystal growth processes from metastable liquids substantiates the importance of studying the various features of these processes and phenomena.

The intermediate stage of phase transformation phenomena occurs when crystals actively appear and evolve in supercooled melts and supersaturated solutions and form a polydisperse ensemble of growing particles. Such an ensemble is described by the particle-size distribution function, the moments of which completely characterize the current state of a metastable system. Note that for the sake of simplicity of the theoretical description, growing particles are usually assumed to be spherical. Taking

---

[a] e-mail: eugenya1m@gmail.com

this into account, the theory of particles evolution was constructed in a series of works [14–20] with allowance for the “diffusion” mechanism of the distribution function in the space of crystal radii. However, these studies do not take into account the shift in the phase transition temperature caused by two effects: (i) the interface curvature or the Gibbs–Thomson effect, and (ii) the attachment kinetics of atoms at the solid-liquid interface. These effects shift the phase transition temperature at the growing surfaces of all particles and, therefore, change the system metastability as well as the distribution function.

Indeed, the phase transition temperature T_i at the solid–liquid interface of a spherical crystal becomes [21,22]

$$T_i = T_* - \frac{\chi}{R} - \frac{1}{\mu_k}\frac{dR}{dt}, \tag{1}$$

where T_* is the phase transition temperature without taking into account the curvature and attachment kinetics, $R(t)$ and t stand for the radius of a growing crystal and time, μ_k is the kinetic coefficient, and $\chi = T_*\alpha/L_V$ (α and L_V represent the coefficient of surface tension and the latent heat parameter).

The boundary-value problem that describes the temperature distribution T around the crystal as well as its radius $R(t)$ and growth rate dR/dt has the form

$$\begin{aligned} \frac{\partial^2 T}{\partial r^2} + \frac{2}{r}\frac{\partial T}{\partial r} &= 0,\ r > R(t), \\ \frac{dR}{dt} = -\frac{\lambda_l}{L_V}\frac{\partial T}{\partial r} &= \beta_*(T_i - T),\ r = R(t), \\ T \to T_l&,\ r \gg R(t), \end{aligned} \tag{2}$$

where r is the radial variable in the spherical coordinate system, β_* is the growth coefficient, λ_l is the thermal conductivity, and T_l is the temperature far from the growing particle. Note that the temperature conductivity equation is written out in the quasi-steady-state approximation when the time derivative $\partial T/\partial t$ is assumed to be small.

Substituting T_i from (1) into (2) and omitting tedious mathematical manipulations, we arrive at the following solution

$$\begin{aligned} \frac{dR}{dt} &= \frac{\tilde{\beta}_*\left(\Delta T - \chi/R\right)}{1 + \tilde{\beta}_* q_T R},\ \tilde{\beta}_* = \frac{\beta_*}{1 + \beta_*/\mu_k},\ \Delta T = T_* - T_l,\ q_T = \frac{L_V}{\lambda_l}, \\ T(r) &= T_l + \frac{\tilde{\beta}_* q_T R^2\left(\Delta T - \chi/R\right)}{\left(1 + \tilde{\beta}_* q_T R\right) r}, \\ t &= \frac{q_T\left(R^2 - R_*^2\right)}{2\Delta T} + \frac{\chi q_T}{\Delta T^2}\left(1 + \frac{\Delta T}{\chi\tilde{\beta}_* q_T}\right)\left(R - R_* + \frac{\chi}{\Delta T}\ln\left|\frac{R\Delta T - \chi}{R_*\Delta T - \chi}\right|\right), \end{aligned} \tag{3}$$

where $R = R_*$ at $t = 0$. Note that the first and second lines of this expression determine the growth rate of a spherical particle and the temperature field around it, whereas the third line describes the radius $R(t)$ in the form of its inverse function $t(R)$. An important point is that all functions dR/dt, T, and t in expressions (3) are parametrically dependent on the liquid supercooling ΔT.

It is significant that the Gibbs–Thomson effect additively decreases the supercooling ΔT in the numerator of the growth rate dR/dt and the effect of attachment kinetics decreases the modified kinetic coefficient $\tilde{\beta}_*$ in comparison with the original kinetic coefficient β_*.

Let us now estimate the contribution induced by the Gibbs–Thomson effect. The radius of nucleating and growing crystals is of the order of [23] $R \gtrsim R_* \gtrsim 10^{-9}$ m. The parameter χ for succinonitrile (SCN), nickel (Ni) and titanium (Ti) can be calculated as [24,25]

$$\chi_{\mathrm{SCN}} = 6.6 \times 10^{-8}\ ,\mathrm{m\,K},\ \ \chi_{\mathrm{Ni}} = 2.1 \times 10^{-7}\,\mathrm{m\,K},\ \ \chi_{\mathrm{Ti}} = 4.2 \times 10^{-6}\,\mathrm{m\,K}.$$

Now estimating ΔT as $\Delta T \lesssim 10^2$ K, we see that the shift χ/R can substantially compensate the supercooling ΔT in the numerator of the growth rate dR/dt. Of course, for crystal growth, shifted supercooling must remain positive. Let us especially note that the growth rate (3) transforms to the previously found expression [9,26–28] in the absence of curvature shift $\chi = 0$.

When considering supersaturated solutions the growth rate dR/dt of an individual crystal induced by the liquid supersaturation ΔC becomes (see, for details, Appendix A)

$$\frac{dR}{dt} = \frac{\tilde{\beta}_* \left(\Delta C - \kappa/R\right)}{1 + \tilde{\beta}_* q_C R \left(1 + \kappa_C/R\right)},\ \tilde{\beta}_* = \frac{\beta_*}{1 + \beta_*/\mu_k}, \tag{4}$$

where β_* and μ_k stand for the growth and kinetic coefficients for the supersaturated solutions, $\kappa = 2C_p\alpha v'/T_*$, C_p is the concentration at saturation for the plane solid/liquid boundary, v' is the molecular volume of solute, T_* is the phase transition temperature for a supersaturated solution, $q_C = C_p(k_0 - 1)/D_l$, k_0 is the equilibrium partition coefficient, D_l is the diffusion coefficient, and $\kappa_C = \kappa/C_p$.

The evolution of a polydisperse ensemble of crystals with allowance for the growth rates dR/dt from expressions (3) and (4) is considered below.

2 A polydisperse ensemble of particles evolving in a supercooled melt

Let a homogeneous metastable melt (solution) has the supercooling ΔT_0 (supersaturation ΔC_0) and does not contain any crystals at the initial moment of time $t = 0$. Introducing the dimensionless supercooling $w = \Delta T/\Delta T_0$ (supersaturation $w = \Delta C/\Delta C_0$), we come to the heat (mass) balance law

$$w(t) = 1 - b \int\limits_{R_*}^{\infty} R^3 \Phi(R,t)dR,\ t > 0, \tag{5}$$

where $b = 4\pi L_V/(3\rho_m C_m \Delta T_0)$ for supercooled melts and $b = 4\pi C_p/(3\Delta C_0)$ for supersaturated liquids. Here, ρ_m and C_m stand for the density and specific heat of a metastable melt.

The particle-radius distribution function $\Phi(R,t)$ satisfies the kinetic equation [14]

$$\frac{\partial \Phi}{\partial t} + \frac{\partial}{\partial R}\left(g\Phi\right) = \frac{\partial}{\partial R}\left(D\frac{\partial \Phi}{\partial R}\right),\ R > R_*,\ t > 0, \tag{6}$$

where $g = dR/dt$, and D is the coefficient of mutual Brownian diffusion of particles in the space of their radii. This coefficient takes the form [14,18]

Table 1. The nucleation rate I and function φ for the Weber–Volmer–Frenkel–Zeldovich and Meirs kinetics corresponding to supercooled melts (subscript sm) and supersaturated solutions (subscript ss), $\varphi_0 = \ln^{-2}\left(1 + w_p^{-1}\right)$, $w_p = C_p/\Delta C_0$. The dimensionless constants I_* and p entering in these expressions are different [26].

	WVFZ kinetics	Meirs kinetics
I_{ss}	$I_* \exp\left[-p \ln^{-2}(C/C_p)\right]$	$I_* \left(\Delta C\right)^p$
I_{sm}	$I_* \exp\left[-p \left(\Delta T_0/\Delta T\right)^2\right]$	$I_* \left(\Delta T\right)^p$
φ_{ss}	$\varphi_0 - \ln^{-2}\left(1 + w/w_p\right)$	$\ln w$
φ_{sm}	$1 - w^{-2}$	$\ln w$

$D = -k_B T g/(dW_{\min}/dR)$. Here, k_B is the Boltzmann constant, and $W_{\min}$ is the minimal work needed to create a crystallite with radius R (for simplicity, we consider the case when $T \approx T_*$).

The natural initial and boundary conditions read as

$$\begin{gathered} \Phi = 0,\ w = 1,\ t = 0;\ \Phi \to 0,\ R \to \infty, \\ g\Phi - D\frac{\partial \Phi}{\partial R} = I(w),\ R = R_*, \end{gathered} \tag{7}$$

where $I(w)$ stands for the nucleation rate (frequency). This rate is equal to the flux of crystallites that overcome the critical energy barrier of nucleation. The nucleation rate is given in Table 1 for two frequently used kinetic mechanisms.

For the sake of simplicity, let us chose the dimensionless parameters and variables as follows:

$$\begin{gathered} t' = \frac{t}{t_0},\ s = \frac{R}{l_0},\ F = l_0^4 \Phi,\ g_0 = \frac{ds}{dt'} = \frac{t_0 g}{l_0},\ D = \frac{d_0 g(t)}{P(R)},\ I_0 = I(1),\ t_0 = \frac{l_0}{\alpha_*}, \\ l_0 = \left(\frac{\alpha_*}{I_0}\right)^{1/4},\ u_0 = \frac{d_0}{l_0},\ s_* = \frac{R_*}{l_0},\ \chi_1 = \frac{\chi}{l_0 \Delta T_0},\ \kappa_1 = \frac{\kappa}{l_0 \Delta C_0},\ \kappa_{C1} = \frac{\kappa_C}{l_0}, \end{gathered} \tag{8}$$

where $\alpha_* = \tilde{\beta}_* \Delta T_0$ for supercooled melts (sm) and $\alpha_* = \tilde{\beta}_* \Delta C_0$ for supersaturated solutions (ss).

Note that $dW_{\min}/dR = -8\pi\alpha(R - R_*)$ near the point $R = R_*$ accordingly to the classical theory developed by Lifshitz and Pitaevskii [14]. By this is meant that $d_0 = k_B T/(8\pi\alpha l_0)$ and $P(R) = (R - R_*)/l_0 = s - s_*$.

Now the kinetic equation (6) can be rewritten as

$$\frac{\partial F}{\partial t'} + g_0 \frac{\partial F}{\partial s} = u_0 g_0 \frac{\partial}{\partial s}\left(\frac{1}{P(l_0 s)}\frac{\partial F}{\partial s}\right),\ s > s_*,\ t' > 0. \tag{9}$$

The crystal growth rate in dimensionless form is defined by expressions

$$\begin{gathered} g_0(t') = \frac{ds}{dt'} = \frac{w - \chi_1/s}{1 + Q_T s},\ \text{sm}, \\ g_0(t') = \frac{ds}{dt'} = \frac{w - \kappa_1/s}{1 + Q_C s\left(1 + \kappa_{C1}/s\right)},\ \text{ss}, \end{gathered} \tag{10}$$

where $Q_T = \tilde{\beta}_* q_T l_0$, $Q_C = \tilde{\beta}_* q_C l_0$, and $s(t')$ can be determined from the corresponding Cauchy problem with allowance for the initial condition $s = s_*$ at $t' = t'_*$ (here t'_* designates the time moment when a spherical nucleus originates).

Further, introducing the modified time (x_1) and spatial (z_1) variables

$$x_1 = \int\limits_0^{t'} g_0\left(t''\right) P\left(l_0 s\left(t''\right)\right) dt'',\ z_1 = \int\limits_0^{z} P_1\left(z''\right) dz'', \tag{11}$$

we rewrite the kinetic equation (9) in the form of

$$\frac{\partial F}{\partial x_1} + \frac{\partial F}{\partial z_1} = u_0 \frac{\partial^2 F}{\partial z_1^2},\ z_1 > 0,\ x_1 > 0, \tag{12}$$

where $z = s - s_*$, and $P_1(z) = P\left(l_0\left(z + s_*\right)\right)$.

Combining expressions (11) with the growth rate $g_0 = ds/dt'$ and $P_1 = z''$, we arrive at the coordinate of particle surface $s(t')$ written out in the form $z_1(x_1) = x_1$ and $z_1 = z^2/2 = (s - s_*)^2/2$.

Keeping this in mind, we rewrite the heat (mass) balance equation (5) as follows

$$w(x_1) = 1 - b \int\limits_{s_*}^{\infty} s^3 F\left(x_1, z_1(s)\right) ds,\ x_1 > 0. \tag{13}$$

It is significant that g_0 can be represented as a function of x_1 with allowance for the dependence $z_1(x_1) = x_1$, i.e.

$$\begin{aligned} g_0(x_1) &= \frac{w(x_1) - \dfrac{\chi_1}{s_* + \sqrt{2x_1}}}{1 + Q_T\left(s_* + \sqrt{2x_1}\right)},\ \text{sm},\\ g_0(x_1) &= \frac{w(x_1) - \dfrac{\kappa_1}{s_* + \sqrt{2x_1}}}{1 + Q_C\left(s_* + \sqrt{2x_1}\right)\left(1 + \dfrac{\kappa_{C1}}{s_* + \sqrt{2x_1}}\right)},\ \text{ss}. \end{aligned} \tag{14}$$

Now keeping in mind that $dx_1/dt' = \sqrt{2x_1} g_0(x_1)$ from (11), we obtain the real dimensionless time t' in terms of the modified time x_1 as

$$\begin{aligned} t'(x_1) &= \int\limits_0^{x_1} \frac{1 + Q_T\left(s_* + \sqrt{2\tilde{x}_1}\right)}{\sqrt{2\tilde{x}_1}\left[w(\tilde{x}_1) - \dfrac{\chi_1}{s_* + \sqrt{2\tilde{x}_1}}\right]} d\tilde{x}_1,\ \text{sm},\\ t'(x_1) &= \int\limits_0^{x_1} \frac{1 + Q_C\left(s_* + \sqrt{2\tilde{x}_1}\right)\left(1 + \dfrac{\kappa_{C1}}{s_* + \sqrt{2\tilde{x}_1}}\right)}{\sqrt{2\tilde{x}_1}\left[w(\tilde{x}_1) - \dfrac{\kappa_1}{s_* + \sqrt{2\tilde{x}_1}}\right]} d\tilde{x}_1,\ \text{ss}. \end{aligned} \tag{15}$$

Expressions (7) in dimensionless form become

$$\begin{gathered} F = 0,\ w = 1,\ x_1 = 0;\ F \to 0,\ z_1 \to \infty,\\ F - u_0 \frac{\partial F}{\partial z_1} = J(x_1) = \frac{\exp\left\{p\varphi[w(x_1)]\right\}}{g_0(x_1)},\ z_1 = 0. \end{gathered} \tag{16}$$

Note that the function $\varphi(w)$ is listed in Table 1 for different kinetic mechanisms frequently met in practice.

The boundary-value problem (12), (16) can be solved using the famous Laplace transform method. The final solution reads as (see, for details, Appendix B)

$$F(x_1, z_1(s)) = \int_0^{x_1} J(x_1 - y_1)\gamma(y_1, z_1)dy_1, \tag{17}$$

where

$$\gamma(y_1, z_1) = \frac{1}{2u_0}\exp\left(\frac{2z_1 - y_1}{4u_0}\right)\left[\frac{2\sqrt{u_0}}{\sqrt{\pi y_1}}\exp\left(\frac{-z_1^2}{4u_0 y_1}\right)\right.$$
$$\left. - \exp\left(\frac{z_1}{2u_0} + \frac{y_1}{4u_0}\right)\operatorname{erfc}\left(\frac{z_1}{2\sqrt{u_0 y_1}} + \frac{\sqrt{y_1}}{2\sqrt{u_0}}\right)\right].$$

Expression (17) determines the particle-radius distribution function, which depends on the metastability degree w [$J(x_1 - y_1)$ depends on w, see expression (16)].

Combining (13) and (17), we come to the following integral equation for w

$$w(x_1) = 1 - b\int_0^{x_1} J(x_1 - y_1)h(y_1)dy_1, \tag{18}$$

where

$$h(y_1) = \int_0^{\infty} \frac{\left(s_* + \sqrt{2\tilde{z}_1}\right)^3 \gamma(y_1, \tilde{z}_1)}{\sqrt{2\tilde{z}_1}} d\tilde{z}_1.$$

Let us now introduce the inverse dependence $y_1(w)$ and replace the variable of integration in expression (18) as

$$w = 1 - b\int_1^{w} \frac{\exp\left[p\varphi\left(\tilde{w}\right)\right]}{G_0\left(\tilde{w}\right)}\frac{dy_1}{d\tilde{w}} h\left[y_1\left(\tilde{w}\right)\right] d\tilde{w},\ \ G_0(w) = g_0 \text{ at } z_1 = 0. \tag{19}$$

Keeping in mind (14), we get

$$G_0(w) = \frac{w - \dfrac{\chi_1}{s_*}}{1 + Q_T s_*},\ \text{sm},$$
$$G_0(w) = \frac{w - \dfrac{\kappa_1}{s_*}}{1 + Q_C s_*\left(1 + \dfrac{\kappa_{C1}}{s_*}\right)},\ \text{ss}. \tag{20}$$

Differentiating (19) with respect to the metastability degree, we come to the differential equation connecting w and y_1. Its integration leads to

$$\int_1^w \frac{G_0\left(\tilde{w}\right)}{\exp\left[p\varphi\left(\tilde{w}\right)\right]} d\tilde{w} = H(x_1) = -b\int_0^{x_1} h(y_1)dy_1. \tag{21}$$

Expression (21) determines w as a function of modified time x_1.

Note that in the case of Meirs kinetics, this equation can be easily evaluated. The final result reads as

$$\begin{gathered}(1-p)\left(w^{2-p}-1\right)-\frac{\chi_1}{s_*}(2-p)\left(w^{1-p}-1\right)=(1-p)(2-p)\Upsilon_T(x_1),\quad p\neq 1,\ p\neq 2,\\ w-1-\frac{\chi_1}{s_*}\ln w=\Upsilon_T(x_1),\ p=1,\\ \ln w+\frac{\chi_1}{s_*}\left(\frac{1}{w}-1\right)=\Upsilon_T(x_1),\ p=2,\\ \Upsilon_T(x_1)=(1+Q_T s_*)H(x_1)\end{gathered} \tag{22}$$

for supercooled melts, and

$$\begin{gathered}(1-p)\left(w^{2-p}-1\right)-\frac{\kappa_1}{s_*}(2-p)\left(w^{1-p}-1\right)=(1-p)(2-p)\Upsilon_C(x_1),\quad p\neq 1,\ p\neq 2,\\ w-1-\frac{\kappa_1}{s_*}\ln w=\Upsilon_C(x_1),\ p=1,\\ \ln w+\frac{\kappa_1}{s_*}\left(\frac{1}{w}-1\right)=\Upsilon_C(x_1),\ p=2,\\ \Upsilon_C(x_1)=\left[1+Q_C s_*\left(1+\frac{\kappa_{C1}}{s_*}\right)\right]H(x_1)\end{gathered} \tag{23}$$

for supersaturated solutions. Let us especially emphasize that expressions (22) and (23) transform to the previously found solution in the limiting case $\chi_1 = 0$, $\kappa_1 = 0$ and $\kappa_{C1} = 0$ [18] when the Gibbs–Thomson effect is not significant.

3 Discussion and conclusion

The exact analytical solution (15), (17) and (22) is shown in Figures 1–4 for the pure titanium melt in the case of Meirs nucleation mechanism. It is easy to see that the melt supercooling w decreases with the growth of modified time x_1 and real dimensionless time t' (Fig. 1). Note that x_1 builds up with increasing t' (Fig. 2). The Gibbs–Thomson and attachment kinetics effects (solid lines) are compared with the case when these effects are not included in the model equations (dashed lines). As is easily seen, these effects lead to slightly faster desupercooling for the melt under consideration. This is clearly seen in Figure 3, where the modified time variable x_1 is eliminated using the dynamical law (15), which is illustrated in Figure 2. As a result, the distribution function, which takes into account the aforementioned effects, is shifted up and to the left (compare the solid and dashed curves in Fig. 4).

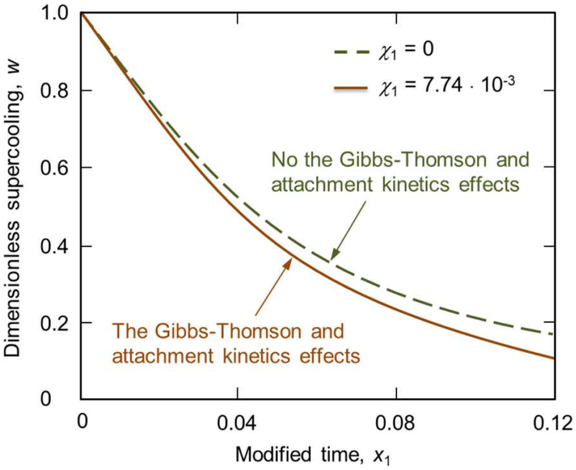

Fig. 1. The dimensionless supercooling w as a function of the modified time x_1. The materials parameters for a single-component Ti melt are [25]: $\Delta T_0 = 300\,\mathrm{K}$, $\beta_* = 10^{-4}\,\mathrm{m\,s^{-1}\,K^{-1}}$, $I_0 = 2.7 \times 10^{21}\,\mathrm{m}^{-3}\,\mathrm{s}^{-1}$, $p = 3$, $u_0 = 10^{-2}$, $s_* = 0.1$, $l_0 = 1.83 \times 10^{-6}\,\mathrm{m}$, $Q_T = 0.91$, $q_T = 4.98 \times 10^9\,\mathrm{K\,s\,m^{-2}}$, $b = 139.06$.

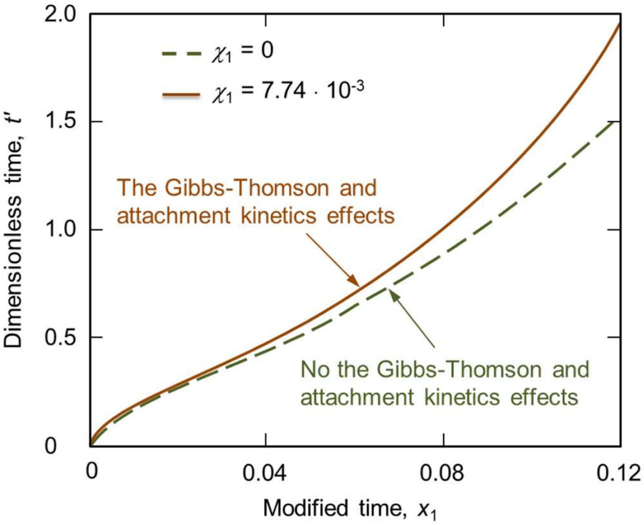

Fig. 2. The dimensionless time t' as a function of the modified time x_1. The materials parameters are the same as in Figure 1.

Indeed, the growth rate dR/dt and the nucleation rate I in the presence of the Gibbs–Thomson effect (see the first expression (3) and the second expression (7)) become lower as compared with the case of no the Gibbs–Thomson temperature shift. As this takes place, the distribution function moves faster to larger crystal radii in the absence of the interface curvature and attachment kinetics effects (the dashed line lies to the right of the solid line for large values of z_1). In addition, the difference between the solid and dashed curves grows with time. Thus, the effects under consideration substantially change the granulometric composition of the supercooled melt.

Let us especially highlight that the tail of the distribution function at large times undergoes essential changes in the presence of the Gibbs–Thomson and attachment

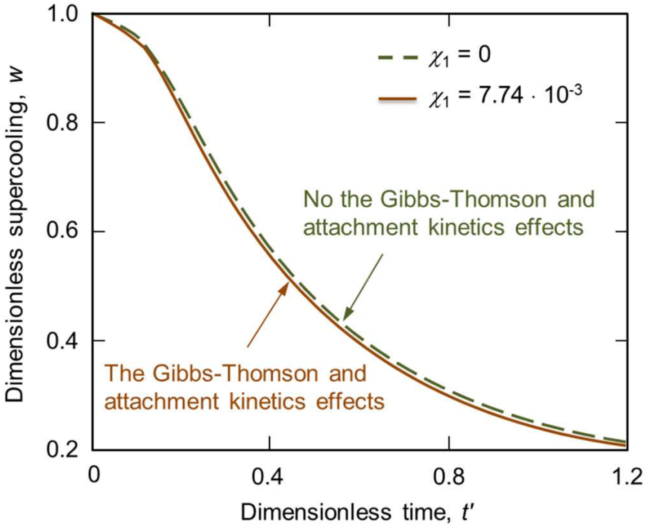

Fig. 3. The dimensionless supercooling w as a function of the real dimensionless time t'. The materials parameters are the same as in Figure 1.

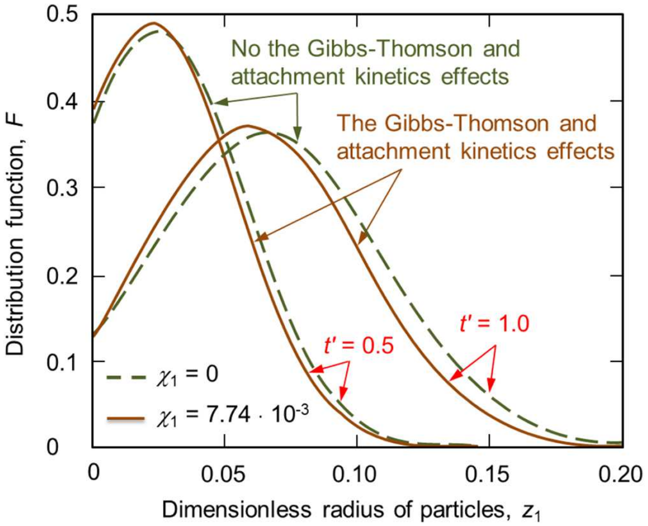

Fig. 4. The dimensionless particle-radius distribution function F versus the dimensionless radius z_1 of crystals at different time moments t'. The materials parameters are the same as in Figure 1.

kinetics effects. It is easily seen by comparing the solid and dashed lines for $t' = 1$ and the large values of dimensionless coordinate z_1. As this tail determines the initial state of the phase transformation process at the concluding stage of Ostwald ripening [30–34], the system behavior at final stages should be studied with allowance for these effects.

It is also important to develop the present theory, taking into account the simultaneous occurrence of the bulk and directional phase transitions in a supercooled two-phase region, where nucleation and growth of crystallites, as well as the evolution of dendrite-like structures, are possible. Such a generalization can be made by analogy with the previously developed theories [35–48].

Appendix A: Evolution of a spherical crystal in a metastable solution

The boundary-value problem that describes the concentration distribution C around the crystal as well as its radius $R(t)$ and growth rate dR/dt has the form

$$\begin{aligned} \frac{\partial^2 C}{\partial r^2}+\frac{2}{r}\frac{\partial C}{\partial r}&=0,\ r>R(t),\\ \frac{dR}{dt}=\frac{D_l}{(k_0-1)C}\frac{\partial C}{\partial r}&=\beta_*(C-C_i),\ r=R(t),\\ C&\to C_l,\ r\gg R(t), \end{aligned}$$

where $C_l=C_p+\Delta C$ is the solute concentration far from the growing particle. Note that the diffusion equation is written out in the quasi-steady-state approximation when the time derivative $\partial C/\partial t$ is assumed to be small. The interfacial concentration C_i is given by [14]

$$C_i=C_p+\frac{\kappa}{R}+\frac{1}{\mu_k}\frac{dR}{dt}.$$

Integrating the diffusion equation and using the far-field boundary condition, we have

$$C(r)=C_l-\frac{C_0}{r}.$$

Substituting this profile into the first boundary condition at $r=R(t)$, we find C_0 in terms of the growth rate $g=dR/dt$ as

$$C_0=\frac{C_l g R}{g+D_l/[R(k_0-1)]}.$$

Its substitution into the second boundary condition at $r=R(t)$ enables us to determine the growth rate. Taking into account that the growth rate g is sufficiently small in the steady-state approximation, we neglect the quadratic term g^2 and come to the following expression

$$g=\frac{dR}{dt}=\frac{\tilde{\beta}_*\left(\Delta C-\kappa/R\right)}{1+\tilde{\beta}_* q_C R\left(1+\kappa_C/R\right)},\ \tilde{\beta}_*=\frac{\beta_*}{1+\beta_*/\mu_k}.$$

Now keeping in mind that

$$C_0=R\left(\Delta C-\frac{\kappa}{R}-\frac{1}{\tilde{\beta}_*}\frac{dR}{dt}\right),$$

we arrive at the concentration distribution around the growing crystal

$$C(r) = C_l - \frac{q_C \tilde{\beta}_* \left(\Delta C - \kappa/R\right) R^2 \left(1 + \kappa_C/R\right)}{\left[1 + \tilde{\beta}_* q_C R \left(1 + \kappa_C/R\right)\right] r}.$$

Further, integrating the growth dR/dt, we obtain the dynamical law $R(t)$ in the form of its inverse function $t(R)$, which reads as

$$t(R) = \int\limits_{R_*}^{R} \frac{1 + q_C \tilde{\beta}_* \Xi \left(1 + \kappa_C/\Xi\right)}{\tilde{\beta}_* \left(\Delta C - \kappa/\Xi\right)} d\Xi.$$

Thus, the aforementioned expressions determine the analytical solutions describing the quasi-steady-state growth of a spherical crystal in the supersaturated solution.

Appendix B: The crystal-size distribution

This Appendix is devoted to the question of how to solve the boundary-value problem (12), (16).

So, applying the Laplace transform to this problem, we obtain

$$F^*(\lambda, z_1) = \frac{2J^*(\lambda)}{1 + \sqrt{1 + 4u_0\lambda}} \exp\left(\frac{1 - \sqrt{1 + 4u_0\lambda}}{2u_0} z_1\right),$$

where the Laplace transform with respect to x_1 is designated by the superscript $*$ (λ stands for the Laplace transform variable).

Inverting this expression with respect to λ, we arrive at the distribution function $F(x_1, z_1)$. To do this, we use the tabulated Laplace transform [29]

$$\frac{\exp\left(-\sqrt{\beta(\lambda + b_1)}\right)}{b_2 + \sqrt{\lambda + b_1}} \to \exp\left(-b_1 x_1\right) \left[\frac{1}{\sqrt{\pi x_1}} \exp\left(-\frac{\beta}{4x_1}\right) \right. \\ \left. - b_2 \exp\left(b_2\sqrt{\beta} + b_2^2 x_1\right) \operatorname{erfc}\left(\frac{\sqrt{\beta}}{2\sqrt{x_1}} + b_2\sqrt{x_1}\right)\right],$$

and obtain the density distribution function

$$F(x_1, z_1) = \exp\left(\frac{z_1}{2u_0}\right) \int\limits_0^{x_1} \frac{J(x_1 - y_1)}{2u_0} \exp\left(\frac{-y_1}{4u_0}\right) \\ \times \left[2\sqrt{\frac{u_0}{\pi y_1}} \exp\left(\frac{-z_1^2}{4u_0 y_1}\right) - \exp\left(\frac{z_1}{2u_0} + \frac{y_1}{4u_0}\right) \operatorname{erfc}\left(\frac{z_1}{2\sqrt{u_0 y_1}} + \frac{\sqrt{y_1}}{2\sqrt{u_0}}\right)\right] dy_1.$$

Here

$$b_1 = \frac{1}{4u_0},\ b_2 = \frac{1}{2\sqrt{u_0}},\ \beta = \frac{z_1^2}{u_0}.$$

This function gives the distribution function (17).

This work was supported by the Russian Science Foundation (grant number 20-61-46013).

References

1. D. Herlach, P. Galenko, D. Holland-Moritz, *Metastable solids from undercooled melts* (Elsevier, Amsterdam, 2007)
2. V.G. Dubrovskii, *Nucleation theory and growth of nanostructures* (Springer, Berlin, 2014)
3. P.K. Galenko, D.V. Alexandrov, Philos. Trans. R. Soc. A **376**, 20170210 (2018)
4. D.V. Alexandrov, A.Yu. Zubarev, Philos. Trans. R. Soc. A **377**, 20180353 (2019)
5. D.V. Alexandrov, A.Yu. Zubarev, Philos. Trans. R. Soc. A **378**, 20200002 (2020)
6. W. Kurz, D.J. Fisher, *Fundamentals of solidification* (Trans. Tech. Publ., Aedermannsdorf, 1989)
7. A.H. Janse, *Nucleation and crystal growth in batch crystallizers* (Delft University of Technology, Delft, 1977)
8. A. Pot, *Industrial sucrose crystallization* (Delft University of Technology, Delft, 1980)
9. I.V. Alexandrova, D.V. Alexandrov, Philos. Trans. R. Soc. A **378**, 20190245 (2020)
10. D.A. Barlow, J. Cryst. Growth **311**, 2480 (2009)
11. D.V. Alexandrov, I.G. Nizovtseva, Philos. Trans. R. Soc. A **377**, 20180214 (2019)
12. I.H. Leubner, J. Disp. Sci. Technol. **23**, 577 (2002)
13. K.F. Kelton, A.L. Greer, *Nucleation in condensed matter: applications in materials and biology* (Elsevier, Amsterdam, 2008)
14. E.M. Lifshitz, L.P. Pitaevskii, *Physical kinetics* (Pergamon, Oxford, 1981)
15. D.V. Alexandrov, Philos. Mag. Lett. **94**, 786 (2014)
16. E.V. Makoveeva, D.V. Alexandrov, Philos. Trans. R. Soc. A **376**, 20170327 (2018)
17. E.V. Makoveeva, D.V. Alexandrov, Philos. Trans. R. Soc. A **377**, 20180210 (2019)
18. D.V. Alexandrov, Phys. Lett. A **378**, 1501 (2014)
19. V.A. Shneidman, Phys. Rev. E **82**, 031603 (2010)
20. V.A. Shneidman, Phys. Rev. E **84**, 031602 (2011)
21. D.V. Alexandrov, P.K. Galenko, L.V. Toropova, Philos. Trans. R. Soc. A **376**, 20170215 (2018)
22. P.K. Galenko, D.V. Alexandrov, E.A. Titova, Philos. Trans. R. Soc. A **376**, 20170218 (2018)
23. V.P. Koverda, V.N. Skokov, V.P. Skripov, Phys. Status Solidi A **74**, 343 (1982)
24. J. Gao, M. Han, A. Kao, K. Pericleous, D.V. Alexandrov, P.K. Galenko, Acta Mater. **103**, 184 (2016)
25. P.K. Galenko, K. Reuther, O.V. Kazak, D.V. Alexandrov, M. Rettenmayr, Appl. Phys. Lett. **111**, 031602 (2017)
26. D.V. Alexandrov, A.P. Malygin, J. Phys. A: Math. Theor. **46**, 455101 (2013)
27. D.V. Alexandrov, I.V. Alexandrova, Philos. Trans. R. Soc. A **377**, 20180209 (2019)
28. D.V. Alexandrov, I.V. Alexandrova, A.A. Ivanov, A.P. Malygin, I.O. Starodumov, L.V. Toropova, Russ. Metall. (Metally) **2019**, 787 (2019)
29. V.A. Ditkin, A.P. Prudnikov, *Integral transforms and operational calculus* (Pergamon Press, Oxford, 1965)
30. V.V. Slezov, J. Phys. Chem. Solids **39**, 367 (1978)
31. V.V. Slezov, *Kinetics of first-order phase transitions* (Wiley, VCH, Weinheim, 2009)
32. D.V. Alexandrov, J. Phys. A: Math. Theor. **48**, 035103 (2015)
33. D.V. Alexandrov, I.V. Alexandrova, Philos. Trans. R. Soc. A **378**, 20190247 (2020)
34. D.V. Alexandrov, J. Phys. Chem. Solids **91**, 48 (2016)

35. R.N. Hills, D.E. Loper, P.H. Roberts, Q. J. Mech. Appl. Math. **36**, 505 (1983)
36. A.C. Fowler, IMA J. Appl. Maths **35**, 159 (1985)
37. V.T. Borisov, *Theory of two-phase zone of a metal ingot* (Metallurgiya Publishing House, Moscow, 1987)
38. A.A. Ivanov, I.V. Alexandrova, D.V. Alexandrov, Philos. Trans. R. Soc. A **377**, 20180215 (2019)
39. D.V. Alexandrov, A.A. Ivanov, I.V. Alexandrova, Philos. Trans. R. Soc. A **376**, 20170217 (2018)
40. R.C. Kerr, A.W. Woods, M.G. Worster, H.E. Huppert, J. Fluid Mech. **216**, 323 (1990)
41. M.G. Worster, J. Fluid Mech. **167**, 481 (1986)
42. D.V. Alexandrov, I.A. Bashkirtseva, L.B. Ryashko, Philos. Trans. R. Soc. A **376**, 20170216 (2018)
43. D.V. Alexandrov, A.P. Malygin, Int. J. Heat Mass Trans. **54**, 1144 (2011)
44. D.V. Alexandrov, Int. J. Heat Mass Trans. **47**, 1383 (2004)
45. A.A. Ivanov, I.V. Alexandrova, D.V. Alexandrov, Eur. Phys. J. Special Topics **229**, 365 (2020)
46. D.V. Alexandrov, Eur. Phys. J. Special Topics **229**, 383 (2020)
47. I.G. Nizovtseva, D.V. Alexandrov, Philos. Trans. R. Soc. A **378**, 20190248 (2020)
48. D.L. Aseev, D.V. Alexandrov, Acta Mater. **54**, 2401 (2006)